# Development of a open-vessel single-stage respirometer

S. Marsili-Libelli, V. D'Ardes and C. Bondi

## ABSTRACT

This paper describes the development and accuracy analysis of a single-stage respirometer which can be used both in the laboratory for wastewater characterization and in the plant as a process instrument. It is based on an accurate model of parasitic aeration, making the two-stage assumption unnecessary. Its operation is supervised by a real-time software, written in Lab View, managing the various measurement procedures and estimating the wastewater characteristics. Its accuracy is assessed through sensitivity and error propagation analysis, proving superior to the conventional model. A laboratory implementation of the instrument was tested with readily degradable substrate, yielding consistent and accurate respirograms.

**Key words** | on-line process control, parameter estimation, respirometry, sensitivity analysis, sensors

**S. Marsili-Libelli**
**V. D'Ardes**
**C. Bondi**
Department of Systems and Computers,
University of Florence,
Via S. Marta 3, I-50139
Florence,
Italy
E-mail: *marsili@dsi.unifi.it*

## INTRODUCTION

Respirometry is a major tool for assessing the viability of a microbial community (Spanjers & Vanrolleghem 1995; Brouwer *et al.* 1998). and provide wastewater treatment plants with accurate on-line information for control (Spanjers *et al.* 1998). One of the main factors affecting the accuracy of conventional two-stage respirometers is the stray air intrusion in the respiration chamber (Marsili-Libelli & Tabani 2002). This paper presents the development of an open-vessel single-stage respirometer where the parasitic (stray) aeration is accounted for and estimated along with the other conventional parameters, producing a low-cost robust instrument which can be used for field and control studies. The identifiability of the instrument model is assessed using the approach outlined in Marsili-Libelli & Tabani (2002); Marsili-Libelli *et al.* (2003) and Checchi & Marsili-Libelli (2005).

## STRUCTURE OF THE RESPIROMETER

In the present version, the instrument is composed of a respiration vessel with aerator and stirrer (see Figure 1). The DO probe is inclined to minimize the entrapment of ascending air bubbles. The DO meter (OXI 90, WTW, Weilheim, Germany) outputs an analogue signal which is 16-bit digitized by an ADAM 4018 (Advantech, Cincinnati, OH, USA) analogue-digital converter communicating with the local PC via a RS-485 serial line through a protocol converter RS_485/RS-232 (ADAM 4520). The instrument is operated by a real-time control software developed in the Lab View 6.1™ platform (National Instruments, Austin, TX, USA), which provides the necessary functionalities for system monitoring, air switching and on-line parameter estimation.

The instrument can be operated either in the switching mode, turning the aeration on and off, or in the RODTOX mode (Vanrolleghem *et al.* 1990) with a single sweep, obtaining in either case the responses of Figure 2. In the former mode two criteria may be applied: the switching may be driven by two DO threshold or a fixed OFF time can be set. The former choice has the advantage of producing the same amount of samples for each cycle.

## RESPIROMETER MODEL

The uncontrolled (stray) air diffusion from the head space of the respiration vessel into the solution is a major source of

doi: 10.2166/wst.2008.149

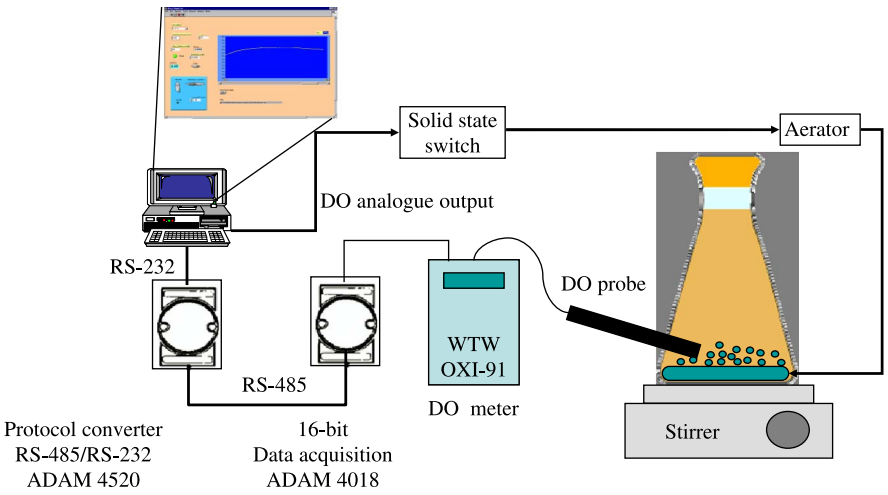


**Figure 1** | Structure of the open-vessel, single-stage respirometer described in this paper. The instrument is supervised by a real-time control software developed in Lab View® 6.1.

error (Marsili-Libelli & Tabani 2002). The result is the loss of linearity in the dissolved oxygen (DO) decay. To account for this effect, the respiration model is rewritten as

$$\frac{dC}{dt} = K(C_{sat} - C) - r \text{ with } K = \begin{cases} K_L a + K_L a_p & \text{ON} \\ K_L a_p & \text{OFF} \end{cases} \quad (1)$$

where $C$ is the dissolved oxygen concentration (mg/L), $r$ is the oxygen uptake rate (mg/L.s), $K_L a$ (1/s) is the oxygen transfer through the aerator and $K_L a_p$ (1/s) represent the stray oxygen transfer coefficient. During the OFF phase, oxygen transfer is not entirely discontinued due to the stray aeration. Equation (1) can be solved analytically for either phase from the initial condition $C_o$ to obtain

$$C(t) = \underbrace{C_o(0)e^{-K\cdot t}}_{\substack{\text{effect of} \\ \text{initial conditions } C_o}} + \underbrace{\left(C_{sat} - \frac{r}{K}\right)}_{\text{forced response}}(1 - e^{-K\cdot t}) \quad (2)$$

From Equation (2) it appears that during the respiration cycle the DO follows an exponential curve and the departure from linearity is directly proportional to the stray oxygen transfer rate $K_L a_p$, as shown in Figure 3.

If the respiration rate $r$ is constant during the single respiration cycle of Figure 3, the DO concentration tends to the constant value

$$C_{reg} = \left(C_{sat} - \frac{r}{K}\right) \quad (3)$$

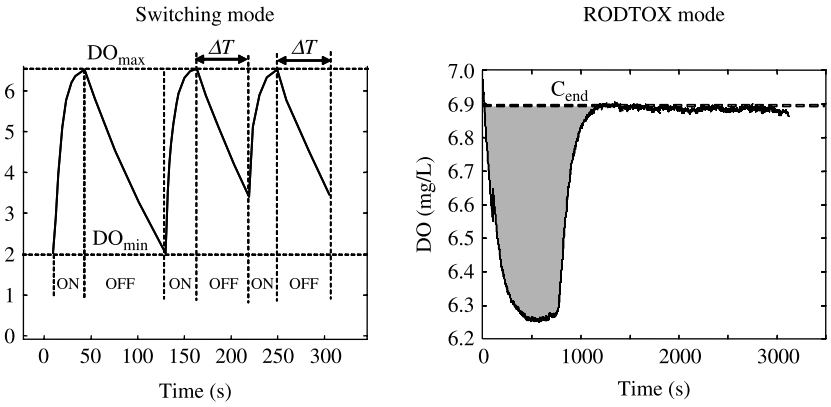


**Figure 2** | The two possible operating modes of the instrument: cyclic switching mode driven by DO thresholds or fixed timing (left) or single- pass RODTOX mode with continuous aeration (right).

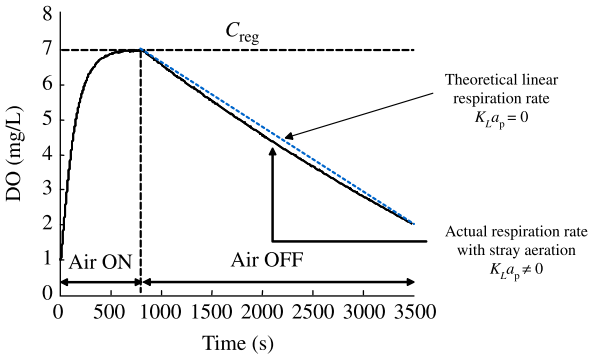


**Figure 3** | Experimental respiration curve showing the loss of linearity in the descending part due to stray air diffusion. The dashed line represents the ideal linear DO decay without this disturbance.

which holds strictly for nonzero aeration, because if $K \rightarrow 0$ then $Creg \rightarrow -\infty$.

## Structural identifiability of the respirometric model

Applying the Pohjanpalo test (Vanrolleghem *et al.* 1995) to the model (2)

$$\begin{cases} \frac{dC}{dt}(0) = -K\cdot\left(C_0 - C_{sat} + \frac{r}{K}\right) = v_1 \\ \frac{d^2C}{dt^2}(0) = K^2\cdot\left(C_0 - C_{sat} + \frac{r}{K}\right) = v_2 \\ \frac{d^3C}{dt^3}(0) = -K^3\cdot\left(C_0 - C_{sat} + \frac{r}{K}\right) = v_3 \end{cases}$$

$$\Rightarrow \begin{cases} K = -\frac{v_2}{v_1} = \sqrt{\frac{v_3}{v_1}} \\ C_{sat} = C_0 - \frac{v_1}{v_2}\cdot(r + v_1) \end{cases} \Rightarrow C_{sat} = C_o - K(r + v_1) \qquad (4)$$

results in a linear relationship among parameters, hence the model (2) is not structurally identifiable. On the other hand, if the estimation is split in two, identifying $C_{reg}$ and $K = K_L a + K_L a_P$ during the ON phase, whereas the respiration rate $r$ and the parasitic aeration rate $K_L a_P$ are identified during the OFF phase, then each of these two models is structurally identifiable. In fact, reparametrization of the ON model yields the following Pojhanpalo equations

$$\begin{cases} \frac{dC}{dt}(0) = K\cdot(C_{reg} - C_0) = v_1 \\ \frac{d^2C}{dt^2}(0) = -K^2\cdot(C_{reg} - C_0) = v_2 \end{cases} \Rightarrow \begin{cases} K = -\frac{v_2}{v_1} \\ C_{reg} = C_0 - \frac{v_1}{v_2} \end{cases} \qquad (5)$$

which are linearly independent. A similar test proves the identifiability of the OFF model.

## Practical identifiability

The practical identifiability of the model (2) can also be assessed via the sensitivity functions and the Fisher Information Matrix (FIM) (Dochain & Vanrolleghem 2001) in relation to the estimation error functional $J(P)$

$$J(P) = \sum_i q_i\cdot(C_i(P) - C_i^{exp})^2 \qquad (6)$$

where $C_i$ and $C_i^{exp}$ are time-indexed model and experimental DO values and $q_i$ a weight which is assumed as a constant $1/\sigma^2$ in the sequel, with $\sigma$ being the DO measurement accuracy. The FIM

$$F = \frac{1}{\sigma^2}\left[\sum_i \left(\frac{\partial C_i}{\partial P}\right)^T \times \left(\frac{\partial C_i}{\partial P}\right)\right] \qquad (7)$$

is a combination of the output sensitivity functions $\partial C_i/\partial P$, whereas the measurement noise variance can be estimated from the data as $\sigma^2 = (1/(N - n_p))\cdot J(\hat{P})$. Considering the basic parametrization $P = [C_{sat}, r, K]^T$, with $K = K_L a + K_L a_p = K_L a + K_L a_p$, the FIM was computed using a set of about 500 experimental data (a typical respirogram length, with 1 s sampling time) the measurement uncertainty was estimated as $\sigma^2 = 6.93 \times 10^{-4}$. Analysis of the eigenvalues revealed a considerable ill-conditioning, denoting poor identifiability and thus confirming the previous Pojhampalo results. Further, Reich & Zinke (1974) proposed another method to assess the lack of identifiability, based on the redundancy matrix $R$

$$R = D^{-1}\cdot F\cdot D^{-1} \qquad (8)$$

where $D = \mathrm{diag}\left(\sqrt{F_{1,1}}, \sqrt{F_{2,2}}, \sqrt{F_{3,3}}\right)$ is the similarity matrix between the FIM and $R$. The criterion requires the computation of $\det(R^{-1})$ and considers the model ill identifiable if this quantity is greater than $10^3$–$10^4$. This analysis confirmed the lack of identifiability of the original model. Conversely, the reduced parametrization of the ON model $P_{ON} = [C_{reg}, K]^T$ yields a better conditioned FIM. In particular, the ratio $\lambda_{max}/\lambda_{min}$ is eleven orders of magnitude smaller that the previous one. It should be reminded that

the extreme eigenvalue rato is equal to the mod ($E$), one of the most used optimal experiment design criteria used in Marsili-Libelli *et al.* (2003) and Checchi & Marsili-Libelli (2005). The redundancy matrix test yields a result well below the threshold set by Reich & Zinke (1974). The comparison of the identifiability parameters for the two parametrizations is summarized in Table 1. It can be concluded that the reparametrization had a beneficial effect on identifiability.

Further, visual inspection of the sensitivity trajectory of the reparametrized model, in Figure 4, show that a long ON period is beneficial for estimating $C_{reg}$ but not for $K$, which has a sensitivity peak shortly after the start of the aeration. Likewise, in the OFF phase the estimation accuracy of $r$ and $K_L a_p$ increases almost linearly with the phase length.

## Computation of parameter uncertainty

The FIM can be used to compute the parameter covariance matrix $C$ as $F^{-1}$ (see e.g. Dochain & Vanrolleghem 2001). For the two models, with the original and reduced parametrization $C$ is computed as

$$C = \begin{pmatrix} 5.62\times10^{4} & 6.83\times10^{2} & -4.44\times10^{-10} \\ 6.83\times10^{2} & 8.29 & 1.23\times10^{-10} \\ -4.44\times10^{-10} & 1.23\times10^{-10} & 1.08\times10^{-10} \end{pmatrix} \qquad (9)$$

$$C_1 = \begin{pmatrix} 1.16\times10^{-6} & -7.61\times10^{-9} \\ -7.61\times10^{-9} & 1.09\times10^{-10} \end{pmatrix}$$

showing that the reduced model is more accurate. Further, the uncertainty for $C_{reg}$ in the reduced model is ten orders of magnitude lower than in the original one and lower than the observed DO variance $\sigma^2 = 6.93 \times 10^{-4}$. Hence estimating $C_{reg}$ with the model is more accurate than measuring it directly through DO measurements. Also, measuring $C_{reg}$ implies keeping the DO level high, which can be detrimental both for the probe and the biomass in the respirometer. As a last step, the correlation matrix of the two parametrizations are computed

$$\Gamma = \begin{pmatrix} 1 & 0.99 & -1.79\times10^{-7} \\ 0.99 & 1 & 4.08\times10^{-6} \\ -1.79\times10^{-7} & 4.08\times10^{-6} & 1 \end{pmatrix} \qquad (10)$$

$$\Gamma_1 = \begin{pmatrix} 1 & -0.67 \\ -0.67 & 1 \end{pmatrix}$$

showing much less correlation in the reduced model. In fact, while in the traditional model, $C_{sat}$ and $r$ are highly correlated, and $K$ is almost uncorrelated, in the reduced one the residual ($C_{reg}$, $K$) correlation is due to the fact that the steady-state oxygen concentration depends on $K$.

This analysis demonstrated the advantage of using the partitioned model with the reduced parametrization during the aerated phase. The next step is to evaluate the accuracy with which the original parameters [$C_{sat}$, $r$, $K_L a$, $K_L a_p$] can be computed back.

**Table 1** | Summary of the identifiability results for the two models

| Identifiability indicator | Basic model | Reparametrized model |
|---|---|---|
| det (F) | $5.82 \times 10^{5}$ | $6.99 \times 10^{9}$ |
| tr (F) | $2.41 \times 10^{7}$ | $1.17 \times 10^{7}$ |
| $\lambda_{max}/\lambda_{min}$ (mod E) | $1.79 \times 10^{15}$ | $1.98 \times 10^{4}$ |
| det ($R^{-1}$) | $2.33 \times 10^{11}$ | 1.84 |

## Error propagation and estimation accuracy of the original model parameters

In the previous section it was concluded that the reparametrized model in which $C_{reg}$ and $K$ are estimated during the air ON phase, and $r$ and $K_L a_P$ in the air OFF phase is better identifiable than the conventional model in which all the parameters are jointly estimated.

Now the next step is to evaluate the estimation error of the original (secondary) parameters from that of the (primary) parameters in the two sub-models, provided that these can be obtained from the primary ones with a negligible error.

A Monte Carlo experiment was performed by generating a set of 700 simulated respirograms with perturbed model parameters around their mean value with a gaussian noise of variance comparable to that of the experimental estimations. This set of noisy data was

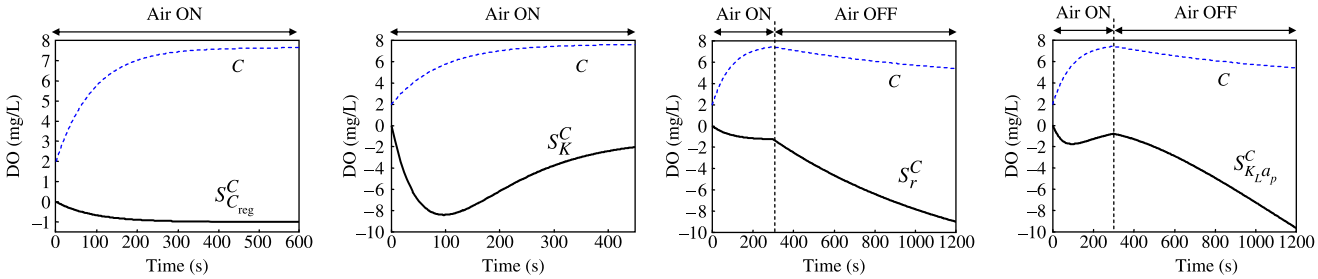


**Figure 4** | Sensitivity trajectories of the reparametrized model obtained with optimal perturbation factors. The left figures refer to the air ON model, whereas the two right ones to the air OFF model.

used to calibrate the primary parameters $P_{ON} = [C_{reg}, K]$ and $P_{OFF} = [r\ K_La_p]$.

Assuming that the primary parameters can be expressed as a mean value and a zero-mean random error

$$\begin{cases} C_{reg} = \bar{C}_{reg} + e_{C_{reg}} \\ K = \bar{K} + e_K \\ r = \bar{r} + e_r \\ K_La_P = \overline{K_La_P} + e_{K_La_P} \end{cases} \tag{11}$$

the propagation of these errors to the secondary parameters

$$K_La = K - K_La_P \quad \text{and} \quad C_{sat} = C_{reg} + \frac{r}{K} \tag{12}$$

can be computed as

$$\begin{aligned} K_La &= \bar{K} + e_K - \overline{K_La_P} - e_{K_La_P} \\ &= (\bar{K} - \overline{K_La_P}) + (e_K - e_{K_La_P}) \end{aligned} \tag{13}$$

$$C_{sat} = \overline{C_{reg}} + e_{C_{reg}} + \frac{\bar{r} + e_r}{\bar{K} + e_K}. \tag{14}$$

From the random simulations the following values were obtained

$$\begin{cases} \bar{\mu}_{K_La} = \bar{\mu}_K - \bar{\mu}_{K_La_P} \cong 10^{-8} - 10^{-6} \cong -10^{-6} \\ \sigma^2_{K_La} = \sigma^2_K + \sigma^2_{K_La_P} \cong 10^{-13} + 10^{-10} \cong 10^{-10} \end{cases} \tag{15}$$

where the most important aspect is that the estimation of $K_La$ is affected by the error on $K_La_P$, whereas the estimation error of $K$ has a negligible influence, being two orders of magnitude smaller.

In the same way, the estimation error of $C_{sat}$ can be evaluated considering $e_K \ll \bar{K}$ to obtain

$$\begin{aligned} C_{sat} &= \overline{C_{reg}} + e_{C_{reg}} + \frac{\bar{r}}{\bar{K}} + \frac{e_r}{\bar{K}} = \left(\overline{C_{reg}} + \frac{\bar{r}}{\bar{K}}\right) + \left(e_{C_{reg}} + \frac{e_r}{\bar{K}}\right) \\ &= \overline{C_{sat}} + e_{C_{sat}} \end{aligned} \tag{16}$$

with mean and variance given by (using again the values obtained from the Monte Carlo simulations)

$$\bar{\mu}_{C_{sat}} = \bar{\mu}_{C_{reg}} + \frac{1}{\bar{K}} \cdot \bar{\mu}_{OUR} \cong 10^{-5} + \frac{1}{10^{-2}} \cdot 10^{-5} \cong 10^{-3} \tag{17}$$

$$\sigma^2_{C_{sat}} = \sigma^2_{C_{reg}} + \frac{1}{\bar{K}^2} \cdot \sigma^2_{OUR} \cong 10^{-8} + \frac{1}{10^{-4}} \cdot 10^{-8} \cong 10^{-4}, \tag{18}$$

which confirm the importance of the magnitude of the mass transfer in adversely affecting the estimation accuracy of $C_{sat}$.

Table 2 compares the estimation accuracy for the basic and reparametrized models, from which it can be concluded that the latter model can be estimated with lower relative errors.

**Table 2** | Comparison of relative estimation errors ($e_r$) of the two models

| Parameter | Basic model | Reparametrized model |
|---|---|---|
| $C_{sat} \approx 7.5$ | $e_r \approx 10^{-1}$ | $e_r \approx 10^{-3}$ |
| $r \approx 10^{-3}$ | $e_r \approx 10^{-1}$ | $e_r \approx 10^{-2}$ |
| $K_La \approx 10^{-2}$ | $e_r \approx 10^{-1}$ | $e_r \approx 10^{-3}$ |
| $K_La_p \approx 10^{-4}$ | $e_r \approx 10^{-2}$ | $e_r \approx 10^{-2}$ |

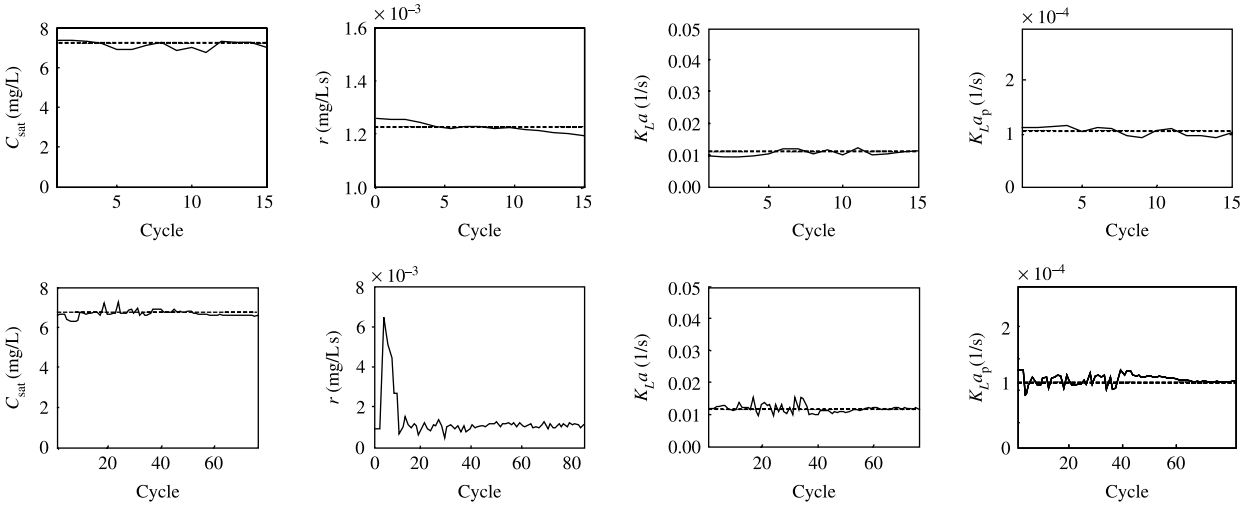


**Figure 5** | Parameter estimation with the basic model in endogenous (above) and growth (below) conditions. The noise level of the estimates is still considerable, especially that on $K_La_p$ The synthesis respirogram was obtained with a small injection of sodium acetate.

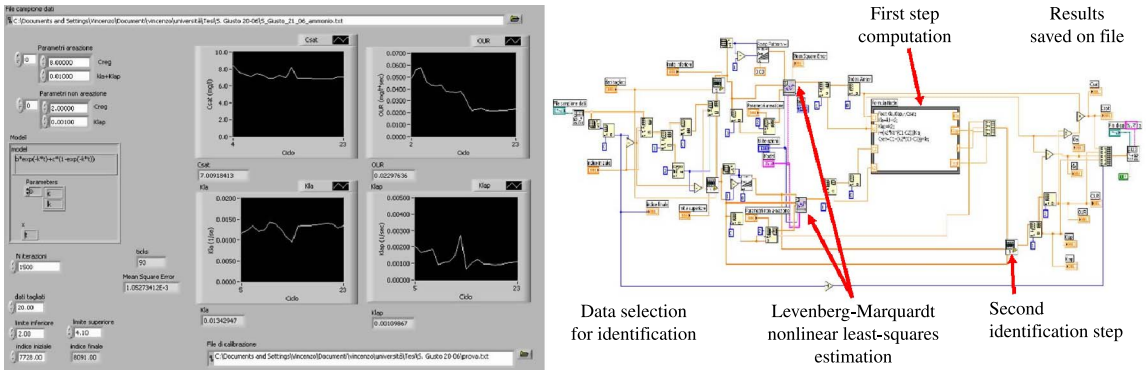


**Figure 6** | Lab View implementation of the respirometer. The graphical user interface (front panel), in which the use can input the experimental conditions, is shown on the left, whereas the operational diagram performing the computation is shown on the right.

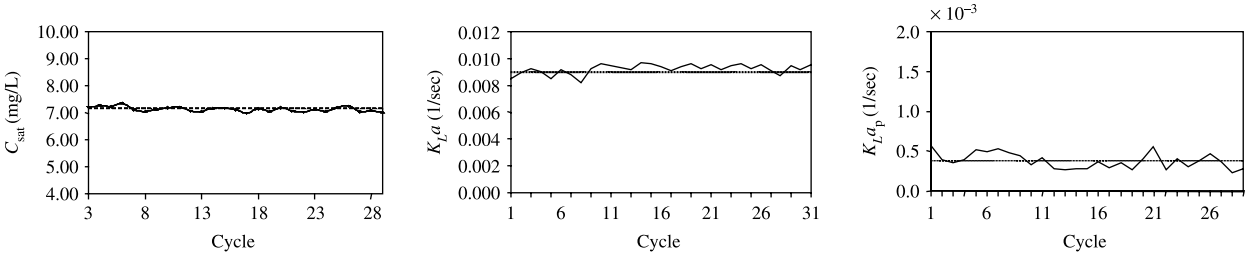


**Figure 7** | Endogenous respiration estimation using the reparametrized model and the implementation of Figure 6.Notice the lower noise level affecting the estimates. The lower $K_La$ value compared with that of Figure 5 is a consequence of a differing air diffusion system.

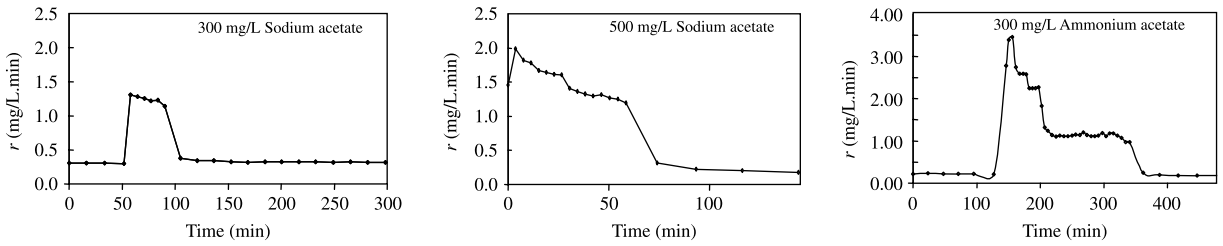


**Figure 8** | Respirograms obtained with the reparametrized model on differing substrate. Notice the lower noise in the endogenous level and the nitrification double-step following the injection of sodium acetate (right). The large datagap in the middle figure could have been avoided with the constant ΔT sampling mode.

## SOFTWARE IMPLEMENTATION AND PERFORMANCE EVALUATION

The software controlling the respirometer was developed in the Lab View 6.1 platform. In the first implementation, the basic respiration model was used and the estimation results are shown in Figure 5. It can be seen that the noise affecting the estimates is still considerable, as a consequence of directly using the basic parametrization. A second implementation was then developed, using the reparametrized model and splitting the estimation in two steps. Depending on the current operating phase (air ON or OFF) the data are routed to the pertinent section, where a nonlinear Levenberg-Marquardt least-squares estimation is performed. Then the original parameters are computed back and the results are written on the hard disk as an ASCII file. The front panel and diagram of the Lab View Virtual Instrument supervising the respirometer is shown in Figure 6. A first application of the improved instrument was to re-estimate the endogenous respiration parameters, as shown in Figure 7, where a better accuracy compared to Figure 5 was obtained, as expected from the previous analysis. The discrepancy between the $K_La$ values depend on a modified aeration system, since the original one proved too powerful and stimulated an excessive development of filamentous bacteria. Later, several respirograms were produced, using readily degradable substrates, either carbonaceous (sodium acetate) or mixed nitrogen/carbon (ammonium acetate). Figure 8 shows three of these respirograms, where the stability of the endogenous level can be appreciated.

## CONCLUSIONS

A single-stage low-cost respirometer was developed for laboratory and process control applications. It is composed of a single open vessel equipped with magnetic stirrer, air diffuser and oxygen probe. The core of the instrument is represented by the Lab View-based software supervising the instrument operation (ON/OFF air switching) and performing on-line parameter estimation. The main idea is to account for stray air infiltration and estimate this uncontrolled input along with normal operating parameters. To improve the estimation accuracy, a reparametrized model was used, whose accuracy proved to be better than that of the conventional one. Later, the implementation aspects have been discussed, showing the instrument laboratory use with test injections. The next step will be an outdoor implementation with remote data acquisition for process control use. From the practical viewpoint, a reliable estimation provides better information for control and the more accurate estimates are in themselves an added bonus because they provide direct information about the biomass metabolic state. Further, the estimation of $K_La_p$, though around 1% of $K_La$, makes the whole estimation scheme more robust and is therefore instrumental in providing a reliable operation.

## REFERENCES

Brouwer, H., Klapwijk, A. & Keesman, K. J. 1998 Identification of activated sludge characteristics using respirometric batch-experiments. *Water Res.* **32**(4), 1240–1254.

Checchi, N. & Marsili-Libelli, S. 2005 Reliability of parameter estimation in respirometric models. *Water Res.* **39**, 3686–3696.

Dochain, D. & Vanrolleghem, P. A. 2001 *Dynamical Modelling and Estimation in Wastewater Treatment Processes*. IWA Publishing, London.

Marsili-Libelli, S. & Tabani, F. 2002 Accuracy analysis of a respirometer for activated sludge dynamic modelling. *Water Res.* **36**, 1181–1192.

Marsili-Libelli, S., Guerrizio, S. & Checchi, N. 2003 Confidence regions of estimated parameters for ecological systems. *Ecol. Model.* **165**, 127–146.

Reich, J. G. & Zinke, I. 1974 Analysis of kinetic and binding measurements. *Studia Biophysica* **43**(2), 91–107.

Spanjers, H. & Vanrolleghem, P. A. 1995 Respirometry as a tool for rapid characterisation of wastewater and activated sludge. *Water Sci. Technol.* **31**(2), 105–114.

Spanjers, H., Vanrolleghem, P. A., Olsson, G. & Dold, P. L. 1998 *Respirometry in Control of the Activated Sludge Process: Principles. (IAWQ Scientific and Technical Report no 7)* IWA Publishing, London.

Vanrolleghem, P. A., Dries, D. & Verstraete, W. 1990 RODTOX: Biosensor for rapid determination of the biochemical oxygen demand and the on-line monitoring of the toxicity of wastewaters. In: *Proceedings Fifth European Congress on Biotechnology*. Copenhagen, Denmark, July 8–13 1990. Vol. 1, 161–164.

Vanrolleghem, P. A., Van Daele, M. & Dochain, D. 1995 Practical identifiability of a biokinetic model of activated sludge respiration. *Water Res.* **29**, 2561–2570.